

## LETTER TO THE EDITOR

# RGS12 inhibits the progression and metastasis of multiple myeloma by driving M1 macrophage polarization and activation in the bone marrow microenvironment

Dear Editor,

Multiple myeloma (MM) is a malignant plasma cancer that grows in the bone marrow and migrates through the bloodstream. Fifty-eight percent of MM patients exhibit the phenotype of hepatomegaly, and 40% have myeloma cell infiltration in the liver [1]. The occurrence and migration of MM are highly associated with the bone marrow microenvironment [2]. A key in the development of MM is the evasion and suppression of the host immune system. Monocyte/macrophage-lineage cells are major components of the infiltrating leukocytes in tumors. Macrophages regulate tumors through not only phagocytosis but also the production of various cytokines and chemokines [3]. Macrophages can be polarized into M1 and M2 macrophages as a reaction to specific microenvironmental stimuli and signals. M1 macrophages are capable of producing numerous cytokines, expressing major histocompatibility complex (MHC), and killing tumor cells. In contrast, M2 macrophages promote angiogenesis, tissue remodeling, and tumor growth [4]. Regulator of G Protein Signaling 12 (RGS12) is a multifunctional protein that is highly expressed in macrophages compared to other

immune cells in the blood and bone marrow cells (Supplementary Figure S1) and is associated with immune signaling [5]. Interestingly, RGS12 was found to have a close relationship with MM during histone deacetylase inhibitor (HDACi) treatment [6]. Therefore, we aimed to investigate the function of macrophage RGS12 in the progression of MM and to identify the potential regulatory mechanisms, all of which may have potential therapeutic relevance in MM and other cancers.

To better understand the pathogenesis of MM and develop new therapeutics, mouse MM models were established in Cre control (Cre recombinase, Ctrl) and RGS12 conditional knockout (cKO) mice. Macrophage-specific RGS12 cKO mice were generated by crossing RGS12-floxed mice with LysM-Cre transgenic mice (Supplementary Figure S2A). Loss of the RGS12 protein in bone marrow macrophages (BMMs) was confirmed by immunoblot analysis of RGS12 cKO mice (Supplementary Figure S2B). RGS12 cKO mice were viable and had no differences in body length or weight compared with control mice (Supplementary Figure S2C-D). To generate the MM model, mouse myeloma cells (MPC-11 cells) were directly injected into the bone marrow through intratibial injection in control (Ctrl, LysM-Cre) and RGS12 cKO (LysM-Cre; RGS12<sup>fl/fl</sup>) mice on the C57BL/6J background (Figure 1A) [7]. After two weeks, typical MM phenotypes were observed in the control and RGS12 cKO mice, including increased osteolytic lesions (Figure 1B and C), a high percentage of B220-CD138<sup>+</sup> cells in the bone marrow (Supplementary Figure S3A), and high serum IgG2b and IgM levels (Supplementary Figure S3B). Moreover, the RGS12 cKO mice exhibited more severe phenotypes than the control mice with MM (Figure 1B and C and Supplementary Figure S3). Most strikingly, the number of liver masses was significantly increased in RGS12 cKO mice compared to control mice by macroscopic and histological analyses (Figure 1D and E). The number of CD138/Ki67-positive cells in the liver was increased in RGS12 cKO mice with MM

**Abbreviations:** MM, Multiple myeloma; MHC, Major histocompatibility complex; RGS12, Regulator of G Protein Signaling 12; HDACi, Histone deacetylase inhibitors; HDAC, Histone deacetylase; Ctrl, Control; KO, Knockout; cKO, Conditional knockout; BMMs, Bone marrow macrophages; PCR, Polymerase chain reaction; Cre, Cre recombinase; FL/FL, Flanked by loxP; WB, Western blot; IP, Immunoprecipitation; B220, B cell isoform of 220 kDa; CD138, Cluster of differentiation 138; Bax, BCL2 associated X; BCL-2, B-cell lymphoma 2; IgG, Immunoglobulin G; IgG2b, Immunoglobulin G2b; IgM, Immunoglobulin M; ELISA, Enzyme-linked immunosorbent assay; BMMs, Bone marrow macrophages; LC-MS/MS, liquid chromatography-tandem mass spectrometry; DAVID, Database for annotation, visualization and integrated discovery; GO, Gene ontology; EP300, E1A binding protein P300; LPS, Lipopolysaccharide; IFN $\gamma$ , Interferon gamma; IL1 $\beta$ , Interleukin 1 $\beta$ ; IL4, Interleukin 4; IL12, Interleukin 12; IL13, Interleukin 13; CD86, Cluster of differentiation 86; CD163, Cluster of differentiation 163

This is an open access article under the terms of the [Creative Commons Attribution-NonCommercial-NoDerivs](https://creativecommons.org/licenses/by-nc-nd/4.0/) License, which permits use and distribution in any medium, provided the original work is properly cited, the use is non-commercial and no modifications or adaptations are made.

© 2021 The Authors. *Cancer Communications* published by John Wiley & Sons Australia, Ltd. on behalf of Sun Yat-sen University Cancer Center

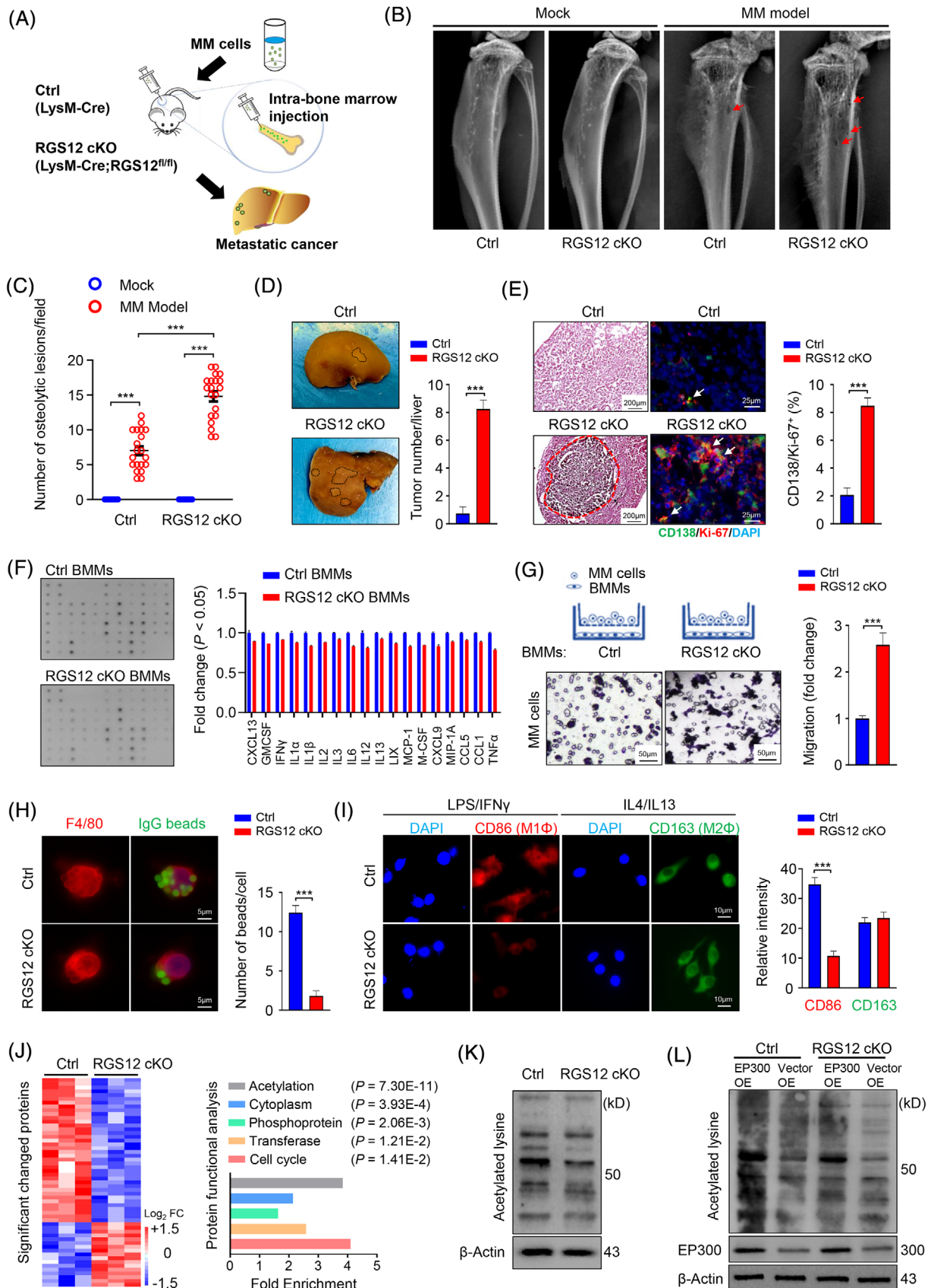


**FIGURE 1** RGS12 in macrophages inhibits the progression and liver metastasis of MM by regulating the bone marrow microenvironment. (A) Mouse model of MM (intra-bone marrow injection). MM cells were cultured in DMEM for 24 hours and injected into the bone marrow through the left anterior tuberosity of the tibia to establish the model of MM in Ctrl (LysM-Cre) and RGS12 cKO (LysM-Cre;

compared with control mice (Figure 1E), suggesting that RGS12 cKO could lead to early and severe liver metastasis of MM. Previous reports have shown that highly metastatic cancer cells exhibit greater resistance to apoptosis [8]. To determine the apoptotic activity in MM liver lesions and bone marrow, the activity of Caspase 3 was detected. The results showed that Caspase 3 activity was significantly decreased in RGS12 cKO liver and bone marrow tissues (Supplementary Figure S4A). Interestingly, we also found that the level of the proapoptotic gene *Bax* was decreased but that of the antiapoptotic gene *Bcl-2* was increased in liver and bone marrow tissues from RGS12 cKO mice compared with those from control mice with MM (Supplementary Figure S4B-C).

To further explore the function of macrophage RGS12 in MM, we harvested BMMs from control and RGS12 cKO mice. BMM lysates were analyzed using an inflammatory cytokine ELISA array. We found that most inflammatory factors were decreased in RGS12 cKO BMMs (Figure 1F), suggesting that RGS12 played a key role in regulating the production of inflammatory factors. To examine

whether macrophages with RGS12 cKO affect the migration of myeloma cells, we seeded control or RGS12 cKO BMMs in the bottom chamber and MM cells in the top chamber of a Transwell system and analyzed the number of migrating MM cells. As a result, the BMMs with RGS12 cKO significantly promoted the migration of MM cells in comparison to the control BMMs (Figure 1G).

Macrophages migrate to and phagocytose microorganisms following activation by inflammatory mediators, such as cytokines and chemokines produced by activated immune cells or tumor cells [9]. To determine whether RGS12 regulates phagocytosis, we obtained RGS12 cKO BMMs and presented IgG-coated fluorescent microbeads to the BMMs as described [10]. As shown in Figure 1H, RGS12 cKO reduced the phagocytic capacity of macrophages by 6.89-fold. Macrophages exhibit phenotypic plasticity in response to microenvironmental changes [4]. We found that RGS12 cKO inhibited the polarization of M1 macrophages (labeled by CD86) under LPS/IFN $\gamma$  induction (Figure 1I) but did not affect the polarization of M2 macrophages (labeled by CD163) under IL4/IL13 induc-

RGS12<sup>fl/fl</sup>) mice. Liver cancer metastasis was determined by histology and biochemical analysis after two weeks. (B) X-ray showing the tibias of Ctrl and RGS12 cKO mice inoculated with/without MM cells by intra-bone marrow injection after 2 weeks. The Ctrl and RGS12 cKO MM model mice showed extensive osteolytic lesions compared to mock control mice (red arrows). (C) The panel shows the number of osteolytic lesions as indicated in (B). Note that the osteolytic lesions were significantly increased in RGS12 cKO mice with MM in comparison to control mice ( $n = 20$ ,  $***P < 0.001$ ). (D) Increased tumor masses in the liver in RGS12 cKO mice with MM. The black circles indicate liver masses. The bar graph shows the numbers of liver masses in Ctrl and RGS12 cKO mice with MM.  $***P < 0.001$ ,  $n = 10$ . (E) HE-stained sections of liver tissues from the Ctrl and RGS12 cKO groups. The red line shows a metastatic lesion. Scale bar, 200  $\mu\text{m}$ . Merged immunofluorescence image showing Ki-67- and CD138-positive cells (white arrows). Green, CD138; red, Ki-67, blue, nuclear DNA (DAPI). Scale bar, 25  $\mu\text{m}$ . The bar graph shows the number of Ki-67/CD138-positive cells relative to the total cells in the liver (%).  $***P < 0.001$ ,  $n = 5$ . (F) BMMs were obtained from Ctrl and RGS12 cKO mice. Mouse cytokine array for detection of cytokine expression in the Ctrl and RGS12 cKO BMMs. Quantitative analysis results for the cytokine levels detected in array plates are shown on the right ( $P < 0.05$ ). (G) Schematic diagram of the myeloma cell invasion assay (top). BMMs were obtained from Ctrl and RGS12 cKO mice and seeded in the bottom chamber. The same amount of MM cells was seeded in the top chamber. MM cells were detected at the bottom of the Transwell insert following migration by 0.5% crystal violet staining. Scale bar, 50  $\mu\text{m}$ . The numbers of MM cells were analyzed by ImageJ software.  $***P < 0.001$ ,  $n = 5$ . (H) The loss of RGS12 inhibits the phagocytosis of IgG-coated fluorescent beads. BMMs were harvested from Ctrl and RGS12 cKO mice. The plasma membrane was stained with anti-F4/80 (red), and IgG-coated beads were identified by yellow-green fluorescence. Scale bar, 5  $\mu\text{m}$ . The number of ingested beads per macrophage is quantified in the right panel.  $***P < 0.001$ ,  $n = 5$ . (I) BMMs were obtained from Ctrl and RGS12 cKO mice. The cells were treated with LPS/IFN $\gamma$  or IL4/IL13 for 24 hours. The M1 macrophage marker CD86 and M2 macrophage marker CD163 were detected by immunofluorescence staining. Scale bar, 10  $\mu\text{m}$ . Note that the loss of RGS12 inhibited M1 macrophage polarization.  $***P < 0.001$ ,  $n = 5$ . (J) Heat map for mass spectrometry analysis depicting the significant changes in protein expression between Ctrl and RGS12 cKO BMMs (left). Optimized cutoff thresholds for significantly altered proteins were set at 1.5 log<sub>2</sub>-transformed ratios ( $P < 0.05$ ,  $n = 3$ ). Protein functional analysis to identify biological processes. The significant biological processes are shown with various colors (right). (K) Deletion of RGS12 decreases acetylation. BMM lysates were extracted from Ctrl and RGS12 cKO mice and used to measure acetylation by immunoblotting. Immunoblot quantification is shown in Supplementary Figure S10A. (L) Overexpression of EP300 restores acetylation in BMMs from Ctrl and RGS12 cKO mice. BMMs from Ctrl and RGS12 cKO mice were transfected with pcDNA3.1-EP300 (EP300 OE) or pcDNA3.1-empty (Vector OE) plasmids for 48 hours. Cell lysates were evaluated by western blotting to measure the acetylation and EP300 levels.  $\beta$ -Actin was used as an internal control. Quantitative analysis results for the acetylation levels are shown in Supplementary Figure S10B.

Abbreviations: RGS12, Regulator of G Protein Signaling 12; MM, Multiple myeloma; DMEM, Dulbecco's modified eagle medium; Ctrl, Control; cKO, Conditional knockout; HE, Hematoxylin and eosin; X-ray, X-radiation; CD138, Cluster of differentiation 138; DAPI, 4',6-Diamidino-2-Phenylindole; BMMs, Bone marrow macrophages; M1 $\Phi$ , M1 macrophage; M2 $\Phi$ , M2 macrophage; IgG, Immunoglobulin G; LPS, Lipopolysaccharide; IFN $\gamma$ , Interferon-gamma; IL4, Interleukin 4; IL13, Interleukin 13; CD86, Cluster of differentiation 86; CD163, Cluster of differentiation 163; EP300, E1A binding protein P300; OE, Overexpression

tion in comparison to control RGS12 expression (Figure 1I). Consistently, forced overexpression of RGS12 in BMMs promoted the phagocytic activity of macrophages (Supplementary Figure S5) and M1 macrophage polarization (increased the expression of CD86, IL1 $\beta$ , and IL12) (Supplementary Figure S6).

To further understand the mechanism by which RGS12 regulates MM pathogenesis, we performed liquid chromatography-tandem mass spectrometry (LC-MS/MS) proteomic analysis to profile the dynamics in control and RGS12 cKO BMMs and identified the most significant up- and downregulated proteins (Figure 1J). We performed Gene Ontology (GO) and protein functional analyses to investigate the biological significance (Figures 1J, Supplementary Figure S7 and Supplementary Table S1). The results revealed that acetylation was the most significantly altered process following RGS12 deletion (Figure 1J), and the levels of most of the proteins related to acetylation were decreased (Supplementary Figure S8). We further confirmed that acetylated proteins were decreased in RGS12 cKO BMMs by immunoblotting (Figure 1K). RGS12 was reported to be associated with HDACs [6], which may play a key role in regulating acetylation. Interestingly, our LC-MS/MS data and immunoprecipitation results showed that RGS12 was associated with the histone acetyltransferase P300 (EP300) in BMMs (Supplementary Figure S9). Moreover, overexpression of EP300 promoted acetylation in BMMs, whereas RGS12 cKO inhibited the upregulation of acetylation caused by EP300 (Figure 1L and Supplementary Figure S10). These results suggest that RGS12 may act as an acetylation enhancer of EP300 to regulate the activation of macrophages.

In summary, this study provides the first evidence that RGS12 inhibits the progression and metastasis of MM by regulating M1 polarization, phagocytosis, and macrophage activation in the bone marrow microenvironment. Therefore, these findings demonstrate that RGS12 could be a potential immunotherapy target in MM and metastasis.

## ACKNOWLEDGMENTS

The authors are grateful to Dr. Min Liu (University of Pennsylvania, USA) for technical assistance in intra-bone marrow injection.

## ETHICS APPROVAL AND CONSENT TO PARTICIPATE

All animal studies were performed in accordance with institutional guidelines and with the ethics approval of the Institutional Animal Care and Use Committee (IACUC) of the University of Pennsylvania.

## AVAILABILITY OF DATA AND MATERIALS

Further information and requests for resources and materials should be directed to and will be fulfilled by the Lead Contact, Dr. Shuying Yang ( [shuyingy@upenn.edu](mailto:shuyingy@upenn.edu) ).

## COMPETING INTERESTS

The authors declare that they have no competing interests.

## FUNDING

This work was supported by grants from the National Institute on Aging [NIA] (AG048388); National Institute of Arthritis and Musculoskeletal and Skin Diseases [NIAMS] (AR066101) to S.Yang, and by grants from the Penn Center for Musculoskeletal Disorders (PCMD), NIH/NIAMS P30-AR069619.

## AUTHORS' CONTRIBUTIONS


YGS, HY, YST, NA performed experiments. YSY and YGS analyzed, interpreted the data and wrote the paper. All authors have read and approved the final manuscript.

Gongsheng Yuan<sup>1</sup>

Yan Huang<sup>1</sup>

Shu-ting Yang<sup>1</sup>

Andrew Ng<sup>2</sup>

Shuying Yang<sup>1,3,4</sup> 

<sup>1</sup> Department of Basic and Translational Sciences, School of Dental Medicine, University of Pennsylvania, Philadelphia, PA 19104, United States

<sup>2</sup> Department of Oral Biology, State University of New York at Buffalo, School of Dental Medicine, Buffalo, NY 14214, United States

<sup>3</sup> The Penn Center for Musculoskeletal Disorders, School of Medicine, University of Pennsylvania, Philadelphia, PA 19104, United States

<sup>4</sup> Center for Innovation & Precision Dentistry, School of Dental Medicine, School of Engineering and Applied Sciences, University of Pennsylvania, Philadelphia, PA 19104, United States

Correspondence

Dr. Shuying Yang, Department of Basic and Translational Sciences, School of Dental Medicine, University of Pennsylvania, Philadelphia, PA19104, United States.

Email: [shuyingy@upenn.edu](mailto:shuyingy@upenn.edu)

## ORCID

Shuying Yang  <https://orcid.org/0000-0002-7126-6901>



## REFERENCES

1. Thomas FB, Clausen KP, Greenberger NJ. Liver disease in multiple myeloma. *Arch Intern Med.* 1973;132(2):195-202.
2. Meads MB, Hazlehurst LA, Dalton WS. The bone marrow microenvironment as a tumor sanctuary and contributor to drug resistance. *Clin Cancer Res.* 2008;14(9):2519-26.
3. Guerriero JL. Macrophages: the road less traveled, changing anticancer therapy. *Trends Mol Med.* 2018;24(5):472-89.
4. Sica A, Mantovani A. Macrophage plasticity and polarization: in vivo veritas. *J Clin Invest.* 2012;122(3):787-95.
5. Yuan G, Yang S, Ng A, Fu C, Oursler MJ, Xing L, et al. RGS12 is a novel critical NF-kappaB activator in inflammatory arthritis. *iScience.* 2020;23(6):101172.
6. Mithraprabhu S, Khong T, Spencer A. Overcoming inherent resistance to histone deacetylase inhibitors in multiple myeloma cells by targeting pathways integral to the actin cytoskeleton. *Cell Death Dis.* 2014;5:e1134.
7. Cutrera J, Johnson B, Ellis L, Li S. Intraosseous inoculation of tumor cells into bone marrow promotes distant metastatic tumor development: a novel tool for mechanistic and therapeutic studies. *Cancer Lett.* 2013;329(1):68-73.
8. Glinsky GV, Glinsky VV. Apoptosis and metastasis: a superior resistance of metastatic cancer cells to programmed cell death. *Cancer Lett.* 1996;101(1):43-51.
9. Atri C, Guerfali FZ, Laouini D. Role of human macrophage polarization in inflammation during infectious diseases. *Int J Mol Sci.* 2018;19(6).
10. Das R, Ganapathy S, Settle M, Plow EF. Plasminogen promotes macrophage phagocytosis in mice. *Blood.* 2014;124(5):679-88.

## SUPPORTING INFORMATION

Additional supporting information may be found in the online version of the article at the publisher's website.

**How to cite this article:** Yuan G, Huang Y, Yang S-, Ng A, Yang S. RGS12 inhibits the progression and metastasis of multiple myeloma by driving M1 macrophage polarization and activation in the bone marrow microenvironment. *Cancer Commun.* 2022;42:60–64. <https://doi.org/10.1002/cac2.12228>